Millipore®
Preparation, Separation,
Filtration & Testing Products

Application Note

# Immunomonitoring using the Scepter™ 2.0 Cell Counter and Scepter™ Software Pro

Amedeo Cappione, Ph.D.[1]; Emily Crossley[2]; Nagaraja Thirumalapura, DVM, Ph.D.[3]; and Debra Hoover, Ph.D.[1] [1]Merck; [2]Dept. of Pathology, Dept. Microbiology & Immunology, University of Texas Medical Branch; [3]Dept. of Pathology, University of Texas Medical Branch.

## Abstract

Biological samples such as primary isolates or cultured cells are often heterogeneous mixtures of cells that differ by type and/or function. Such differences in cellular attributes are most commonly determined by multicolor fluorescent antibody detection of cell type-specific surface markers using flow cytometry. Notably, in addition to variations in protein expression, many cell types and physiological states are also uniquely distinguishable on the basis of size alone. The ability to identify population subsets on the basis of phenotypic differences and further determine their relative frequencies (and concentrations) is critical to many aspects of research.

The Scepter™ cell counter combines the ease of automated instrumentation and the accuracy of the Coulter principle of impedance-based particle detection in an affordable, handheld format. The instrument uses a combination of analog and digital hardware for sensing, signal processing, data storage, and graphical display. The precision-made, consumable polymer sensor has a laser-drilled aperture in its cell-sensing zone that enables the instrument to use the Coulter principle to discriminate cell diameter and volume at submicron and subpicoliter resolution, respectively.

Using a sensor with a 40 µm aperture, the Scepter™ cell counter can accurately and precisely count a broad range of cell types, including small cells (> 3 µm in diameter) and peripheral blood mononuclear cells (PBMC)[1]. This paper describes three examples of experiments using the Scepter™ cell counter's sensitive size-discriminating capability to demonstrate rapid, qualitative assessment of individual cell population frequencies in complex cell mixtures.



MERCK

# Example 1: Lymphocyte vs. monocyte subset discrimination in freshly-isolated PBMCs

## Introduction

The human immune system is comprised of cell subsets, with distinct functional profiles, that fight pathogens. The assessment of expression profiles of the various immune cell subsets, such as lymphocytes and monocytes, can help identify molecular signatures that may facilitate research, ranging from translational medicine and prognostic advancements to early decision-making tools in vaccine development. The Scepter™ cell counter, when used in combination with Scepter™ Software Pro, provides a tool for rapid determination of lymphocyte and monocyte concentrations, as well as the relative frequency of these cell types in PBMC isolates.

## Materials and Methods

### Human blood sample prep

Human PBMCs were isolated from whole heparinized blood of healthy donors by Ficoll®-Paque density centrifugation (GE Healthcare). Briefly, 9 mL of blood were diluted to 25 mL with phosphate-buffered saline (1X EmbryoMax® PBS, Merck) and layered over 15 mL of Ficoll®. Samples were centrifuged at 400 x g for 30 minutes with no brake, and the resulting PBMC layer was recovered. The PBMC fractions were washed twice by centrifugation using PBS. After the final spin, cell pellets were resuspended in PBS for sufficient conductivity during Scepter™ cell counting.

### Scepter™ cell counting

The Scepter™ cell counter was used to count samples following the simple on-screen instructions for each step of the counting process. Briefly, the user attaches a 40 µm sensor, depresses the plunger, submerges the sensor into the sample, then releases the plunger drawing 50 µL of cell suspension through the cell-sensing aperture. The Scepter™ cell counter detects each cell passing through the sensor's aperture, calculates cell concentration, and displays a histogram as a function of cell diameter or volume on its screen.

Scepter™ 2.0 software was then used to upload test files from the device and perform subsequent data analysis to determine the concentrations and relative cell frequencies for the lymphocyte and monocyte fractions.

### Guava® easyCyte™ cell counting

10 µL of each PBMC sample was diluted in 190 µL PBS. Samples were then analyzed on a Guava® easyCyte™ HT system to determine the concentrations and relative cell frequencies for the lymphocyte and monocyte fractions.

### Cell viability determination using Guava® ViaCount assay

10 µL of each PBMC sample was mixed with 190 µL ViaCount® assay reagent, and incubated for 5 minutes at room temperature (RT). Viability data were acquired on a Guava® easyCyte™ instrument using Guava® ExpressPro™ software.

### Cell surface staining and subset determination

For each sample, 100,000 PBMCs were resuspended in 100 µL PBS+0.1% bovine serum albumin (BSA). To distinguish the discrete cell subsets present in PBMC samples, they were stained with the following combination of fluorescently-labeled antibodies: CD3-PE (T cells), CD19-Alexa Fluor® 488 (B cells), CD16/CD56-APC (NK cells), and CD14-PECy7 (monocytes) (antibodies all from eBioscience). Singly-stained samples and isotype controls were included with each staining set to ensure proper instrument setup. Samples were incubated at RT for 20 minutes, washed twice with PBS, then resuspended in 200 µL PBS prior to acquisition. Samples were analyzed (3,000 cells/sample well) on a Guava® easyCyte™ HT system using Guava® ExpressPro™ software.

## Results

### Viability assessment of PBMC

Freshly-prepared or frozen PBMC samples consisted of live cells, dead cells, and a considerable amount of cellular debris. The debris component varied with respect to properties inherent to the blood sample as well as the methods of storage and PBMC preparation. To understand the relative proportions of live cells, dead cells, and debris, freshly-isolated PBMC were stained with ViaCount® reagent.

ViaCount® reagent distinguished viable and non-viable cells based on differential permeabilities of two DNA-binding dyes. The cell-permeant nuclear dye stained all nucleated cells, while the cell-impermeant viability dye brightly stained dying cells. Cellular debris was not stained by either dye.

Results from a representative assay are presented in Figure 1A. In this example, more than 95% of the cells were viable. The three components were also distinguishable on the basis of particle size. The histograms in Figure 1B show the distribution of particles in the different fractions as a function of forward scatter, a flow cytometry-based correlate of particle size. While there was some overlap between size distributions of dead cells and debris, the live cells constituted a distinct fraction made up of two differently sized cell types.

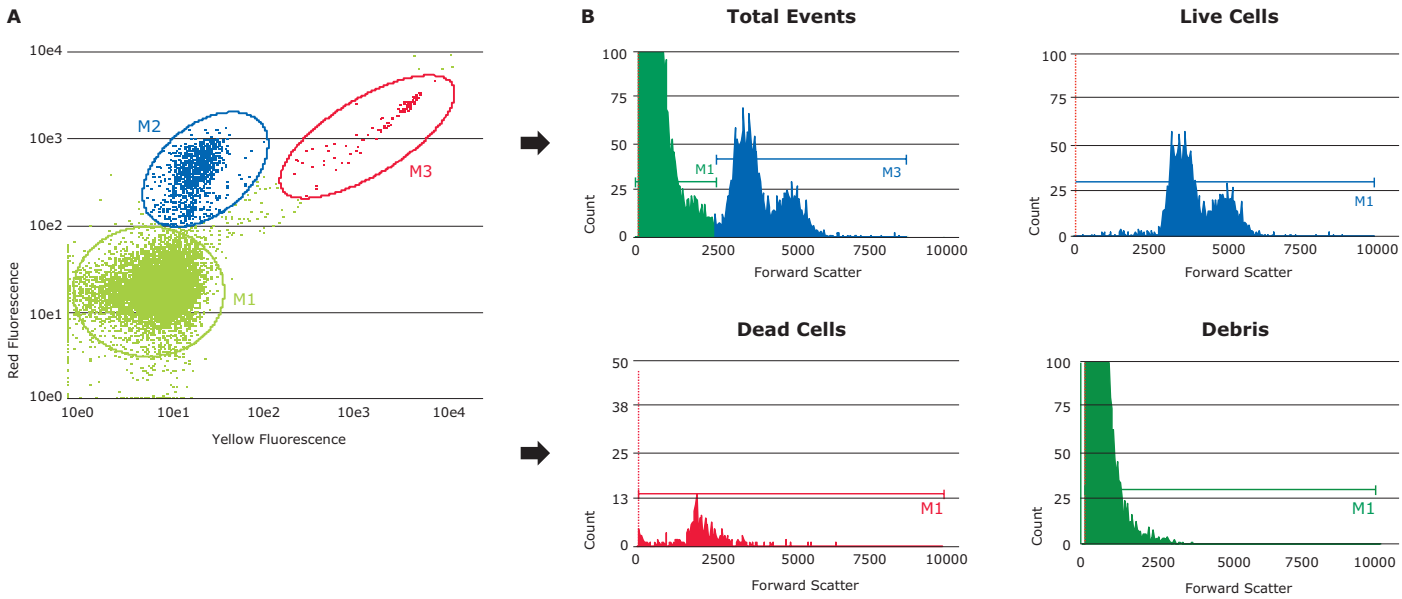


**Figure 1.**

Representative flow cytometry data demonstrating size-based discrimination of live vs dead cells. (A) live cells (blue), dead cells (red), and debris (green) fractions were defined using ViaCount® reagent. (B) The four histograms show the relative distribution of each fraction as a function of particle size (forward scatter).

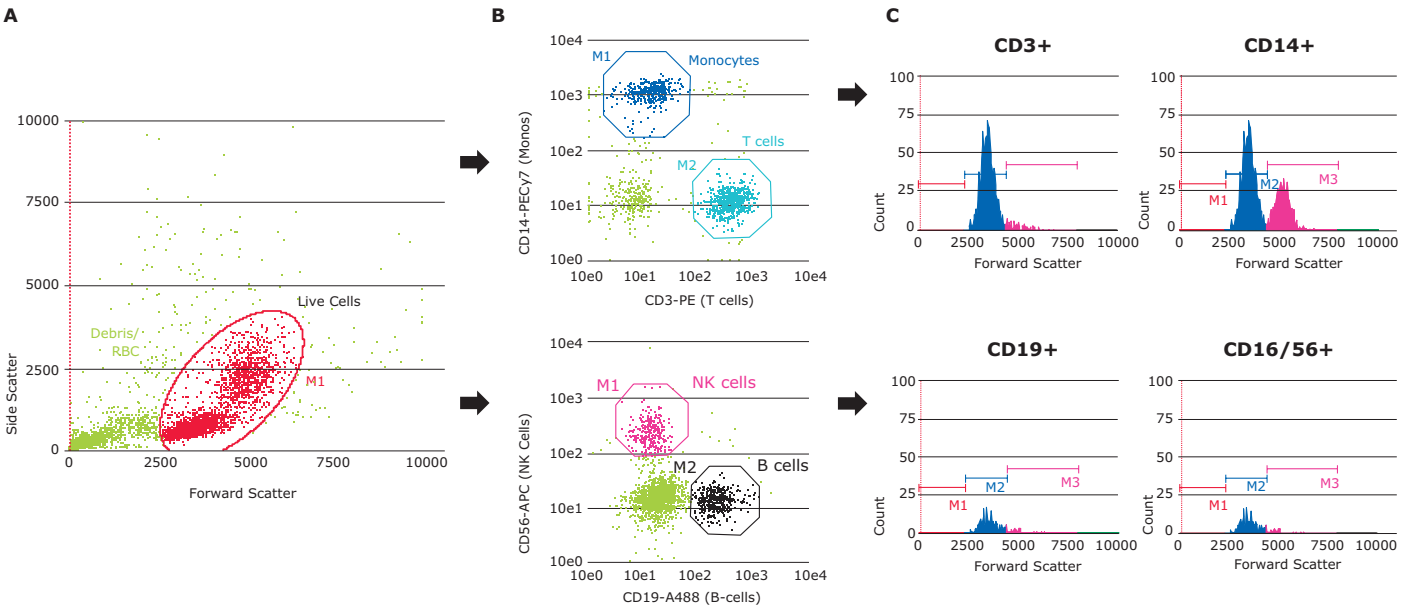


**Figure 2.**

Representative data from flow cytometry analysis of multicolor staining performed on PBMC fractions. (A) Live cells (red) are distinguished from debris/dead cells (green) on the basis of forward vs. side scatter. (B) Live cells from (A) are fractionated in the two plots based on variations in expression of CD14, CD3, CD16/56, and CD19. (C) The four histograms show the localization of each cell fraction with regards to the two peaks defined by forward scatter. As shown, the three major lymphocyte subsets are found predominantly in the smaller-cell peak (blue) while the CD14+ monocytes are restricted to the large-cell fraction (pink).

To investigate the distribution of these four subsets with regard to size, PBMCs were stained with fluorescent antibodies specific for each surface marker (Figure 2). The dot plots confirmed definition of each subset by staining with each cell type-specific marker. Figure 2C demonstrates that B, T, and NK cells were generally smaller in size (low forward scatter) while CD14+ monocytes were larger in size (higher forward scatter).

To examine the ability of the 40 µm Scepter™ sensor to discriminate lymphocytes from monocytes, PBMC fractions were isolated from fresh human blood by Ficoll® gradient centrifugation. Diluted samples were analyzed using both a Guava® easyCyte flow cytometer and the Scepter™ cell counter. Representative histogram plots are presented in Figure 3. In each case, three main peaks were distinguishable by each analysis method, with greater peak resolution in the flow cytometry data, particularly in the separation of lymphocytes from debris. The peaks correspond to lymphocytes (small cells), monocytes (large cells), and a debris/dead cell fraction.

Across the nine PBMC samples analyzed (Table 1), the average mean cell diameters were 7.23±0.30 µm and 10.02±0.20 µm for lymphocytes and monocytes, respectively. Resulting values were consistent with previously reported size ranges[2]. In addition, cell frequencies were determined by three methods: Scepter™ diameter plot, Guava® easyCyte™ forward scatter, and antibody staining. The Scepter™ values slightly underestimated the lymphocyte fraction while overestimating the monocyte subset. This is likely the result of the Scepter™ cell counter's comparatively lower resolution as well as subjectivity and user bias in the placement of gates defining each subset. Overall, there was good agreement between the different analytical techniques with values varying by 10% in nearly all cases.

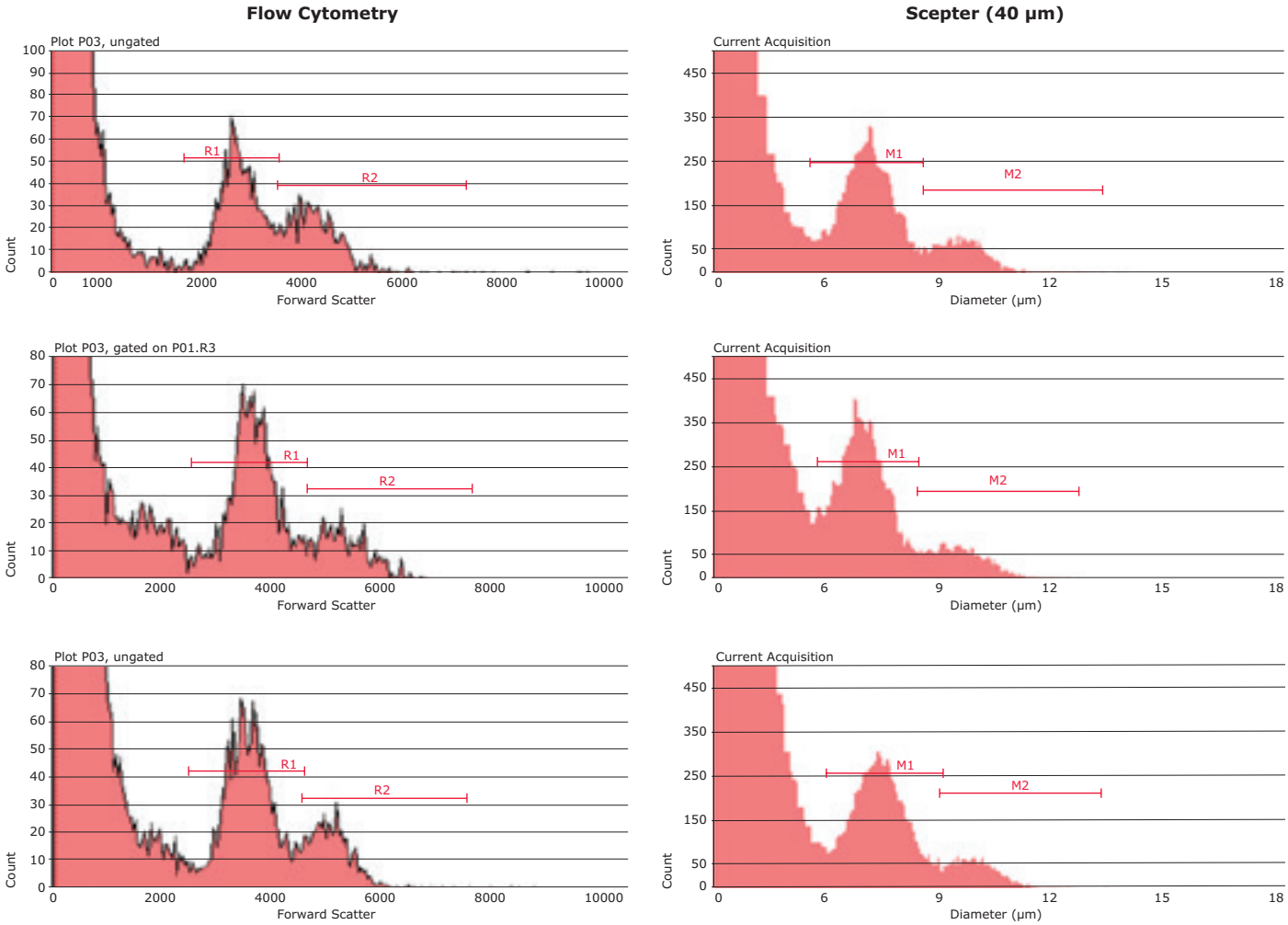


**Figure 3.**

Three representative examples comparing histogram plots for human PBMC samples acquired on the Scepter™ cell counter (diameter readouts on right) and Guava® easyCyte™ flow cytometer (forward scatter figures on left). Analysis plots derived from both platforms demonstrate three distinct peaks corresponding to lymphocyte, monocyte, and dead cell/debris fractions. The difference in cell counts (Y-axis) is attributable to differences in sample dilution between the Guava® flow cytometer and the Scepter™ cell counter.

**Table 1.**

| Test | Cell Fraction | Relative Frequency | | |
|---|---|---|---|---|
| | | Scepter™[1] | Forward Scatter[2] | Staining[3] |
| 1 | Lymphocyte | 58 | 65 | 63 |
| | Monocyte | 42 | 35 | 37 |
| 2 | Lymphocyte | 68 | 72 | 71 |
| | Monocyte | 32 | 28 | 29 |
| 3 | Lymphocyte | 66 | 69 | 71 |
| | Monocyte | 34 | 31 | 29 |
| 4 | Lymphocyte | 62 | 67 | 64 |
| | Monocyte | 38 | 33 | 36 |
| 5 | Lymphocyte | 64 | 66 | 67 |
| | Monocyte | 36 | 34 | 33 |
| 6 | Lymphocyte | 62 | 58 | 60 |
| | Monocyte | 38 | 42 | 40 |
| 7 | Lymphocyte | 65 | 72 | 72 |
| | Monocyte | 35 | 28 | 28 |
| 8 | Lymphocyte | 59 | 61 | 61 |
| | Monocyte | 41 | 39 | 39 |
| 9 | Lymphocyte | 64 | 72 | 72 |
| | Monocyte | 36 | 28 | 28 |

Lymphocyte and monocyte subset frequencies from nine individual PBMC samples. Aliquots from each sample were analyzed using the Guava® easyCyte™ and Scepter™ platforms. [1]Values were derived from the diameter histogram plot. [2]Values were derived from the forward scatter histogram plot based on total events measured on Guava® easyCyte™ platform. [3]Staining frequencies derived as follows: % Leukocytes = % $CD3^+$ T cells+ % $CD16/56^+$ NK+ % $CD19^+$ B cells; % Monocytes = % $CD14^+$ cells.

# Example 2: Human T cell activation

## Introduction

*In vivo,* T lymphocytes are activated and induced to proliferate upon binding of the T cell receptor (TCR) to antigen-presenting cells. In response to stimulation, T cells undergo physical, biological, and phenotypic changes, including increased cell size, secretion of cytokines, and up-regulation of CD25 surface expression, culminating in the production of specifically tuned immune responses. Elevated CD25 expression levels are an indicator of T cell activation[4]. Assays measuring changes in T and B cell activation are commonly used to identify patterns of immune response in clinical diagnostics as well as in the development of therapeutics.

The *in vivo* immune response by T cells can be mimicked *ex vivo* by binding T cells to co-immobilized anti-CD28 and anti-CD3 monoclonal antibodies[3]. PBMCs can also be activated through exposure to more generic inducers of cell proliferation, such as the plant lectin phytohemagglutinin (PHA) or pokeweed mitogen. *Ex vivo* activation enables detailed studies of the molecular mechanisms regulating T cell activation and response.

## Materials and Methods

### Cell culture/activation

Human PBMC fractions were isolated as previously described. Prior to culture, initial cell concentrations were determined using the Scepter™ cell counter. All culturing experiments were performed in RPMI 1640 supplemented with 10% fetal bovine serum (FBS) in the absence of antibiotics. PBMC (400,000 cells/mL, 24-well plates) were stimulated for two days in the presence of soluble anti-CD28 mAb (clone 28.2, BD Pharmingen, 2 µg/mL) on plates pre-coated with anti-CD3 mAb (clone HIT3a; BD Pharmingen, 10 µg/mL). Mitogenic stimulation was carried out in the presence of 2 µg/mL PHA (Sigma). Unstimulated control cultures were also analyzed.

### Scepter™ cell counting

Sample acquisition and data analysis were performed as previously described. Briefly, following stimulation, a small aliquot of each culture was harvested, diluted in PBS, then analyzed on the Scepter™ cell counter. Test files were uploaded and analyzed using Scepter™ Software Pro to determine the degree of cell activation (% activated cells) as well as concentrations for both unstimulated and activated fractions.

## CD25 staining for activation

Following two-day stimulation, cultures were harvested, washed twice with PBS, and then counted using the Scepter™ cell counter. For each sample, 100,000 cells were resuspended in 100 µL PBS+0.1% BSA. To distinguish the activated T cell fraction, samples were stained with anti-CD3-PE (a pan-T cell marker) and anti-CD25-APCeFluor780 (antibodies from eBioscience). Singly-stained samples and isotype controls were included with each staining set to ensure proper instrument setup. Samples were incubated at RT for 20 minutes, washed twice with PBS, then resuspended in 200 µL PBS prior to acquisition. Samples were analyzed (3,000 cells/sample well) on a Guava® easyCyte™ HT system using Guava® ExpressPro™ software.

## Results

To address the potential use of the Scepter™ cell counter for rapid qualitative monitoring of immune cell activation as a function of the cell size shift, freshly-isolated PBMCs were stimulated in culture using two different mechanisms: (1) CD3/CD28 antibody-mediated co-stimulation of the T cell receptor and (2) mitogenic stimulation by PHA.

The dot plots in Figure 4B show three main populations of cells: resting T cell ($CD3^+/CD25^-$), activated T cells ($CD3^+/CD25^+$), and non-T cells ($CD3^-/CD25^-$). Cultures stimulated with CD3/CD28 Ab demonstrated significantly greater levels of T cell activation than those exposed to PHA. Control cultures showed very low frequencies of activated cells. Under all conditions, CD25 expression also correlated with an increase in overall cell size (Figure 4C).

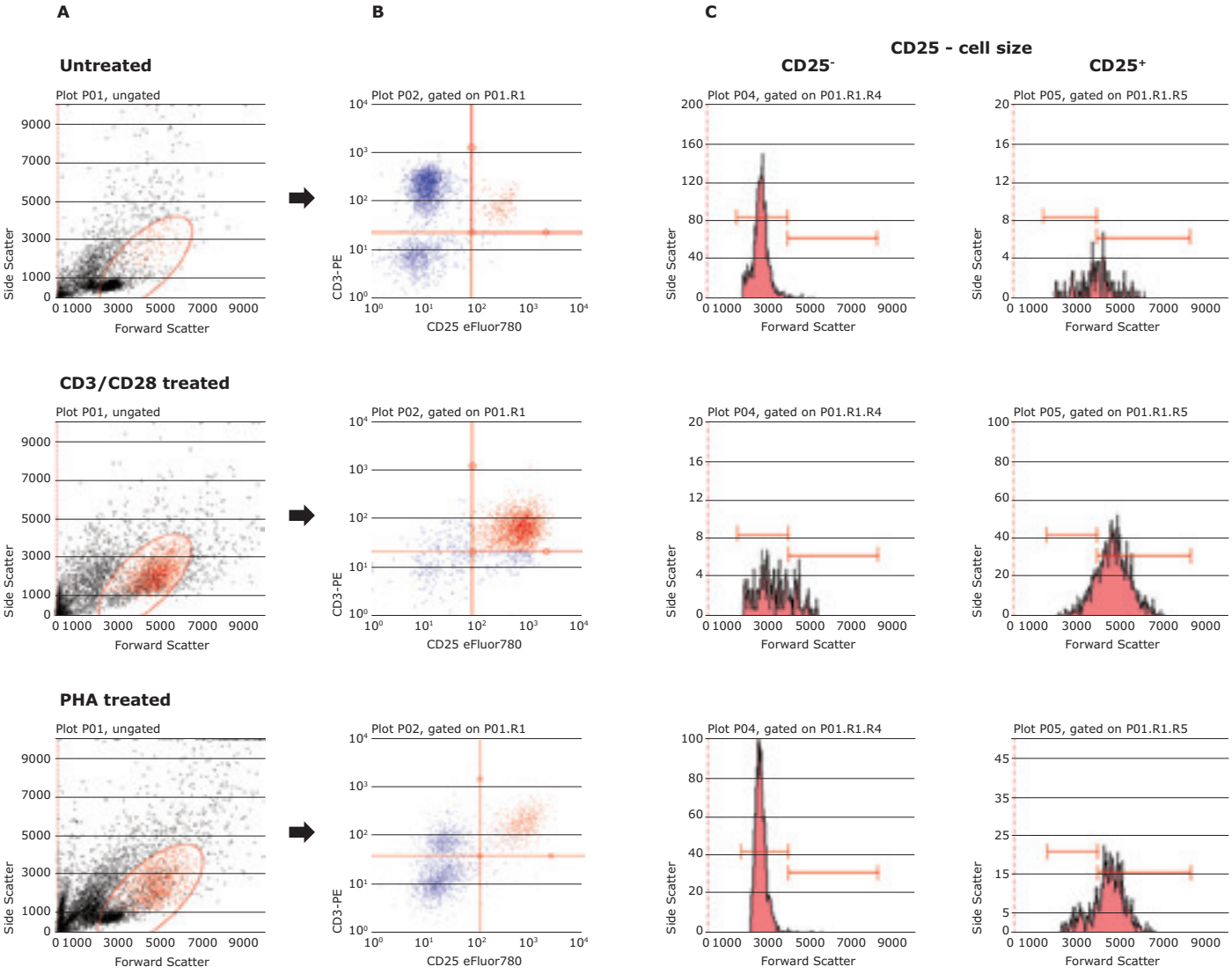


**Figure 4.**

Expression of the cell activation marker CD25 correlates with an increase in cell size. (A) An elliptical gate was used to identify live cells. (B) Dot plots depict the fractionation of live cells on the basis of CD3 and CD25 expression. (C) The forward scatter histogram plots demonstrate that expression of CD25 is restricted to the larger-cell fraction for all culture conditions.

In Figure 5, the Scepter™ cell counter's ability to detect cell activation was compared to that of the Guava® easyCyte™ flow cytometer . While the Scepter™ cell counter was able to detect the presence of the larger, activated cell fraction in both stimulated cultures, the device was unable to simultaneously discriminate the smaller unstimulated population in these samples. This was most likely due to the presence of a large number of dead cells (red cells in Figure 5A) that overlapped in size with the live, unstimulated fraction. This overlap was clearly demonstrated in the untreated sample, in which two peaks were seen in the flow cytometry histogram plot of total cells (Marker R5). By comparison, the live cell-only histogram showed a single peak within R5. The resulting data clearly demonstrated the subset of activated T cells but could not be used to discriminate the live, unstimulated T cell population.

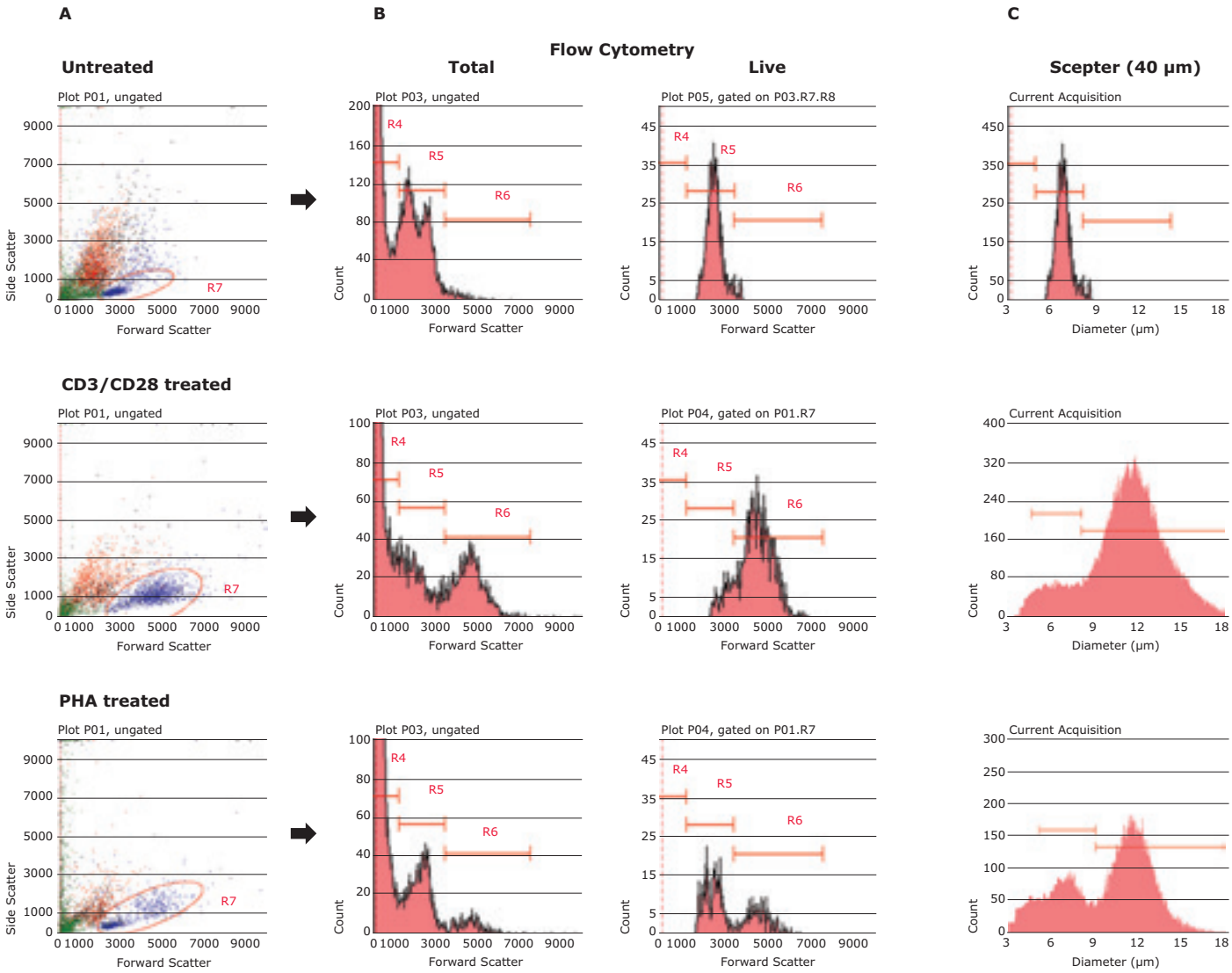


**Figure 5.**

Representative data demonstrating size-based discrimination of resting vs. activated cells in control and stimulated PBMC cultures. (A) Live cell (blue), dead cell (red), and debris (green) fractions were defined using ViaCount reagent. (B) The two histograms in each row show the relative distribution of each fraction as a function of particle size (forward scatter). Plots are based on total events and live cells, respectively. (C) Histogram data for each sample following analysis using the Scepter™ cell counter with 40 µm sensor.

# Example 3: Splenic cell shift in murine model of ehrlichiosis

## Introduction

Human monocytotropic ehrlichiosis (HME) is an emerging tick-borne disease caused by the obligately intracellular pathogen *Ehrlichia chaffeensis* that infects mononuclear phagocytes. HME initially manifests as nonspecific flu-like symptoms but can progress to life-threatening toxic shock-like syndrome with anemia, thrombocytopenia, and multi-organ failure. The presence of extensive inflammation in the absence of bacterial burden suggests that mortality is the consequence of unregulated immunopathology[5,6]. In this study, a murine model of HME based on infection of C57BL/6 mice with *Ehrlichia muris* was used to investigate aspects of the immune response by measuring changes to the population dynamics of splenocytes.

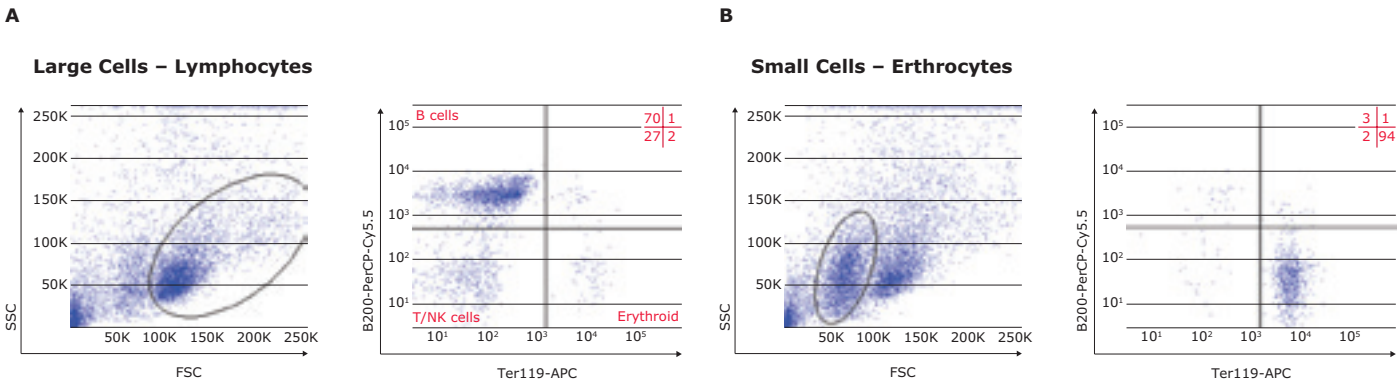


**Figure 6.**

Cell surface staining defines cell subsets within the mouse spleen. Forward vs. side scatter plots reveal the presence of two main splenocyte populations. (A) The fraction containing larger cells is comprised primarily of leukocytes (B, NK, and T cells), while the fraction of small cells (B) is predominantly erythrocytes (TER119$^+$).

## Materials and methods

### Infection of mice with *Ehrlichia muris*

Six- to eight-week-old C57BL/6 mice were infected with *Ehrlichia muris* (~1 x $10^4$ bacterial genomes) by the intraperitoneal route. Mice were sacrificed on day 30 post-infection and spleens were harvested. Single-cell suspensions of splenocytes were prepared using the GentleMACS™ Tissue Dissociator following the manufacturer's instructions (Miltenyi Biotec Inc., CA).

### Determination of splenocyte cell distribution using the Scepter™ cell counter

Cells were diluted to appropriate concentrations (~1 – 2 x $10^5$ cells/mL) and loaded into the Scepter™ cell counter fitted with the 40 µM sensor. The gates were set to exclude red blood cells, using a splenocyte sample from a naïve (uninfected) mouse. Splenocytes from three uninfected mice and three mice infected with *Ehrlichia muris* were used. Data were analyzed using Scepter™ Software Pro.

### Determination of splenocyte cell distribution by flow cytometry

Splenocytes were incubated with a fluorescent viability dye (Near IR LIVE/DEAD™ Fixable Dead Cell Stain Kit, Invitrogen, CA) for 10 minutes in PBS at RT and protected from light. Cells were washed and blocked with Fc Block™ (BD Biosciences, CA) and purified rabbit, rat and mouse IgGs (Jackson ImmunoResearch, PA) in flow cytometry buffer (PBS + 2% FBS + 0.09% sodium azide). Cells were then incubated with fluorescently-labeled antibodies to the surface markers B220 (B cells) and TER119 (erythrocytes) (BD Biosciences, CA and eBioscience, CA, respectively) and analyzed by flow cytometry.

## Results

Single-cell suspensions of mouse splenocytes were analyzed by multicolor flow cytometry (Figure 6). Size-based discrimination using forward scatter confirmed the presence of two distinct cell populations in all samples. Staining with antibodies specific for B cells (B220) and erythrocytes (TER119) demonstrated that erythrocytes were restricted to the subset containing smaller cells, while the fraction of large cells was composed primarily of lymphocytes.

Flow cytometry-derived histograms of total cells showed the presence of three distinct populations corresponding to debris, lymphocytes (large cells) and erythrocytes (small cells). Comparative analysis of splenic cell isolates from *Ehrlichia*-infected and control mice revealed an overall shift in the relative cell distribution. Specifically, infected samples showed an increase in the percentage of erythrocytes when compared to the lymphocyte subset (Figure 7B and Table 2). In contrast, the Scepter™ histogram was able to detect only two peaks; the third peak corresponding to the debris fraction had particle sizes below the lower limit of detection. In addition, the smaller erythrocytes were at the limits of detection for the Scepter™ cell counter and were not counted, skewing the erythrocyte counts. However, the Scepter™ cell counter's quantitation of splenocyte counts and percentages was in very good agreement with the values determined by flow cytometry. An overall assessment of cell concentration values indicated the shift was due to an expansion of the erythrocyte subset in the spleen while lymphocyte values remained constant (Table 3). These findings were consistent with previously published results[7].

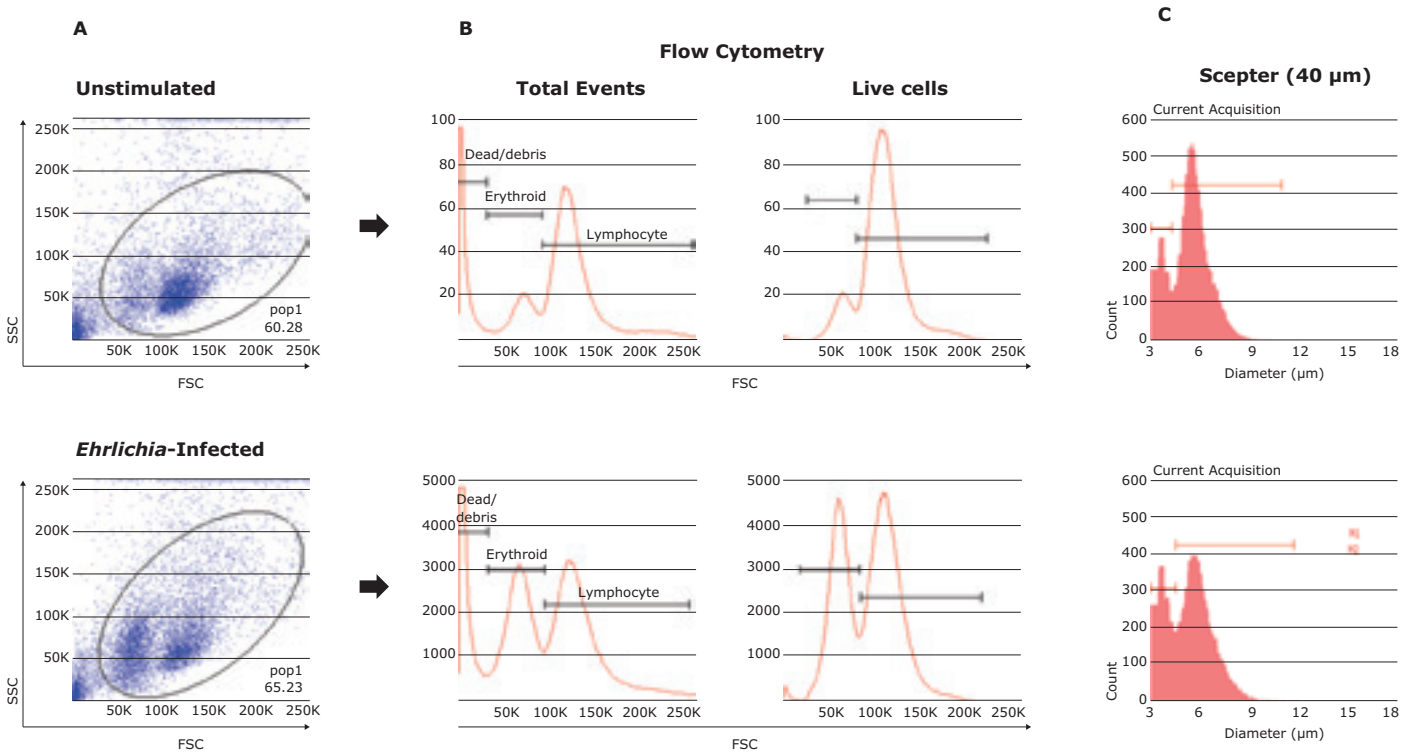


**Figure 7.**

Size-based fractionation of mouse splenocytes. Untreated and *Ehrlichia*-infected samples were analyzed using a flow cytometer (A, B) and using the Scepter™ cell counter (C). Three distinct peaks corresponding to lymphocytes, erythrocytes, and debris can be visualized using flow cytometry. For the Scepter™ cell counter, the particle size of the debris peak is below the level of detection for the 40 µm sensor.

| | Scepter™ | | Flow Cytometry | |
|---|---|---|---|---|
| **Test Sample** | **Erythrocyte** | **Lymphocyte** | **Erythrocyte** | **Lymphocyte** |
| Control - 1 | 27 | 73 | 16 | 84 |
| Control - 2 | 29 | 71 | 21 | 79 |
| Control - 3 | 22 | 78 | 14 | 86 |
| Infected - 1 | 40 | 60 | 42 | 58 |
| Infected - 2 | 30 | 70 | 29 | 71 |
| Infected - 3 | 33 | 67 | 38 | 62 |

**Table 2.**

Total lymphocyte and erythrocyte subset frequencies expressed as percentages of total cell counts from six individual splenocyte isolates (three control, three infected). Aliquots from each sample were analyzed using a flow cytometer and Scepter™ cell counter.

| | Cell Concentration ($x10^5$) | |
|---|---|---|
| **Test Sample** | **Erythrocyte** | **Lymphocyte** |
| Control - 1 | 1.86 | 4.65 |
| Control - 2 | 2.61 | 5.54 |
| Control - 3 | 2.17 | 5.78 |
| Infected - 1 | 4.3 | 5.22 |
| Infected - 2 | 2.82 | 4.93 |
| Infected - 3 | 3.5 | 5.84 |

**Table 3.**

Total lymphocyte and erythrocyte cell concentration for all six samples.

## Overall Conclusions

Evaluation of immune responsiveness to viral, bacterial, cellular and environmental exposure is an important tool in the assessment of pathogenicity and toxicity. The availability of simplified methods for identifying activation status of cells and for measuring differences in the relative frequencies (and concentrations) of more than one cell type in samples or co-cultures is very useful for accelerating research in these fields. We have presented data indicating that both the Guava® easyCyte™ benchtop flow cytometry platform as well as the Scepter™ cell counter can determine such differences in fresh primary isolates and cultured samples. While the flow cytometry system is the more sophisticated and quantitative tool, it requires significant setup, time and operator training. In contrast, the Scepter™ handheld cell counter is a simple tool that can be used at the hood to provide very good insight into cellular responses in as little as 30 seconds. Notably, the Scepter® counter requires no operator training and complements existing methods.

The accuracy and reliability of Scepter™ counting is a function of the precision-engineered sensor and the technical sophistication of the instrumentation that is based upon the Coulter impedance principle. The ability of the Scepter™ device to ensure reproducible cell counts improves data quality during experimental setup and enhances the data credibility of downstream cell-based analyses.

**References**


1. Smith, J. et al. *The New Scepter™ 2.0 Cell Counter Enables the Analysis of a Wider Range of Cell Sizes and Types With High Precision.* Merck Cellutions 2011 Vol. 1: p 19-22.

2. Daniels, V. G., Wheater P.R., Burkitt H.G. *(1979). Functional Histology: A Text and Colour Atlas.* Edinburgh: Churchill Livingstone. ISBN 0-443-01657-7.

3. Prager, E. et al. (2001) *Induction of Hyporesponsiveness and Impaired T Lymphocyte Activation by the CD31 Receptor: Ligand Pathway in T-Cells.* J. Immunol. 166: 2364-2371.

4. Levine, B. L., et al. (1997). *Effects of CD28 Costimulation on Long-term Proliferation of CD4+ T-cells in the Absence of Exogenous Feeder Cells.* J. Immunol. 159:5921 5930.

5. Olano, J. P., G. Wen, H. M. Feng, J. W. McBride, and D. H. Walker. 2004. *Histologic, Serologic, and Molecular Analysis of Persistent Ehrlichiosis in a Murine Model.* Am. J. Pathol. 165:997–1006.

6. Paddock, C. D., and J. E. Childs. 2003. *Ehrlichia chaffeensis: a Prototypical Emerging Pathogen.* Clin. Microbiol. Rev. 16:37–64.

7. MacNamara, K.C., Racine, R. Chatterjee, M., Borjesson, D. and Winslow, G.M. (2009) *Diminished Hematopoietic Activity Associated with Alterations in Innate and Adaptive Immunity in a Mouse Model of Human Monocytic Ehrlichiosis.* Infect. And Immunity. 77:4061-69.

# Ordering Information

### Scepter™ 2.0 Cell Counter

| Description | | Quantity | Cat. No. |
|---|---|---|---|
| **Scepter™ 2.0 Handheld Automated Cell Counter** | with 40 µm Scepter™ Sensors (50 Pack) | 1 | **PHCC20040** |
| | with 60 µm Scepter™ Sensors (50 Pack) | 1 | **PHCC20060** |
| **Includes:** | Scepter™ Cell Counter | 1 | |
| | Downloadable Scepter™ Software | 1 | |
| | O-Rings | 2 | |
| | Scepter™ Test Beads | 1 | **PHCCBEADS** |
| | Scepter™ USB Cable | 1 | **PHCCCABLE** |
| **Scepter™ Sensors, 60 µm** | | 50 | **PHCC60050** |
| | | 500 | **PHCC60500** |
| **Scepter™ Sensors, 40 µm** | | 50 | **PHCC40050** |
| | | 500 | **PHCC40500** |
| **Universal Power Adapter** | | 1 | **PHCCP0WER** |
| **Scepter™ O-Ring Kit, includes 2 O-rings and 1 filter cover** | | 1 | **PHCC0CLIP** |

### Guava® easyCyte™ Benchtop Flow Cytometers

| Description | | Quantity | Cat. No. |
|---|---|---|---|
| **High-Throughput Sampling Instruments Counter** | Guava® easyCyte™ 8HT Base System | 1 | **0500-4008** |
| | Guava® easyCyte™ 6HT/2L Base System | 1 | **0500-4007** |
| | Guava® easyCyte™ 5HT Base System | 1 | **0500-4005** |
| | PCA-96 Base System | 1 | **0100-8710** |
| **Single Sampling Instruments** | easyCyte™ 5 Base System | 1 | **0500-5005** |
| | easyCyte™ 6-2L Base System | 1 | **0500-5007** |
| | easyCyte™ 8 Base System | 1 | **0500-5008** |

## FlowCellect™ Flow Cytometry Assay Kits and Milli-Mark™ Fluorescent Conjugated Antibodies for Immunology

Discover the power of flow cytometry for multiparametric analysis of the immune system: visit **MerckMillipore.com/CellularAnalysis** for complete listings of our fully-validated conjugates and assay kits optimized for Guava® easyCyte™ systems.

| Description | Cat. No. |
|---|---|
| Guava® ViaCount® Reagent | **4000-0041** |
| FlowCellect™ Human Lymphocyte ZAP-70 Characterization Kit | **FCIM025122** |
| FlowCellect™ Mouse FoxP3 Treg Identification Kit | **FCIM025126** |
| Guava® Cell Toxicity Reagents Kit | **4500-0230** |
| FlowCellect™ Human FOXP3 Treg Characterization Kit | **FCIM025118** |
| FlowCellect™ Mouse Th1 Intracellular Cytokine Kit | **FCIM025123** |
| FlowCellect™ Mouse Th2 Intracellular Cytokine Kit | **FCIM025124** |
| FlowCellect™ Mouse Th17 Intracellular Cytokine Kit | **FCIM025125** |
| FlowCellect™ Mouse Th1/Th2 Intracellular Cytokine Kit | **FCIM025137** |
| FlowCellect™ Mouse Th1/TH17 Intracellular Cytokine Kit | **FCIM025138** |

## To place an order or receive technical assistance

In Europe, please call Customer Service:

| | |
|---|---|
| France: 0825 045 645 | Spain: 901 516 645 Option 1 |
| Germany: 069 86798021 | Switzerland: 0848 645 645 |
| Italy: 848 845 645 | United Kingdom: 0870 900 4645 |

For other countries across Europe, please call: +44 (0) 115 943 0840
Or visit: **MerckMillipore.com/offices**
For Technical Service visit: **MerckMillipore.com/techservice**

**MerckMillipore.com**

Merck KGaA
Frankfurter Strasse 250
64293 Darmstadt, Germany

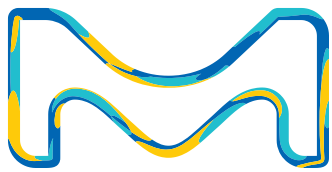



Lit. No. AN3322ENEU Ver. 2.0
2018 - 14316
11/2018